Marquette University
e-Publications@Marquette

Biomedical Engineering Faculty Research and Publications

Biomedical Engineering, Department of

Quasi-Exact Helical Cone Beam Reconstruction for Micro CT

Jicun Hu
Marquette University

Robert C. Molthen
Marquette University, robert.molthen@marquette.edu

Roger Johnson
Marquette University

Steven Haworth
Marquette University

Christopher Dawson
Marquette University

Quasi-exact Helical Cone Beam Reconstruction for Micro CT

J. Hu
Department of Biomed. Engineering, Marquette University, Milwaukee, WI

R. Johnson
Department of Biomed. Engineering, Marquette University, Milwaukee, WI

R. Molthen
Department of Biomed. Engineering, Marquette University, Milwaukee, WI

S. Haworth
Department of Biomed. Engineering, Marquette University, Milwaukee, WI

C. Dawson
Department of Biomed. Engineering, Marquette University, Milwaukee, WI

Abstract: A cone beam micro-CT system is set up to collect truncated helical cone beam data. This system includes a micro-focal X-ray source, a precision computer-controlled X-Y-Z-theta stage, and an image-intensifier coupled to a large format CCD detector. The helical scanning mode is implemented by rotating and translating the stage while keeping X-ray source and detector stationary. A chunk of bone and a mouse leg are scanned and quasi-exact reconstruction is performed using the approach proposed in J. Hu et al. (2001). This approach introduced the original idea of accessory paths with upper and lower virtual detectors having infinite axial extent. It has a filtered backprojection structure which is desirable in practice and possesses the advantages of being simple to implement and computationally efficient compared to other quasi-exact helical cone beam algorithms for the long object problem.

Introduction

In the post genomic sequence era, small animal models (primarily mouse and rat) of important diseases such as hypertension, diabetes and obesity will become increasingly important in functional genomics.[2] Functional geonomics or the Physiome Project is an emerging challenging research area which seeks to link genotypes to phenotypes: genetics to function, Cone beam micro-CT provides a powerful, nontraumatic method to assess phenotypes.

It is well known that cone beam tomography based on FDK approach can only deliver approximate results although it is fast and simple to implement[3] Towards the goal of producing an exact volume reconstruction, cone beam computed tomography (CT) based on nonplanar orbits has been an active area of research. Circle and line, circle and arc, two perpendicular circles and helix are the four complete orbits that researchers have been investigating. The helical scanning mode is preferred in practice because it is natural for fast volumetric scanning of long objects. Exact helical cone beam reconstruction was not practical until researchers found that if the cone beam projection is measured within the region (8) bounded on the detector by the projections of the adjacent upper and lower turns of the helix, then the object can be exactly reconstructed.[4,5] The region B is called the Tam window or *PI* window. This discovery made it possible to do exact reconstruction from truncated data.

Exact helical cone beam tomography algorithms can be categorized as addressing the short object problem or the long object problem. For the short object problem; the axial extent of the helix is sufficient to cover the entire object, providing adequate data for a comparatively simple solution. For the more complex long object problem, the helix extends only slightly beyond the ROI. It is a much more difficult problem to solve than the short object problem due to the data contamination issue. However, the long object problem is more useful in practice. In clinical imaging, only a portion of the patient should be scanned to provide accurate images of the finite volume of interest.
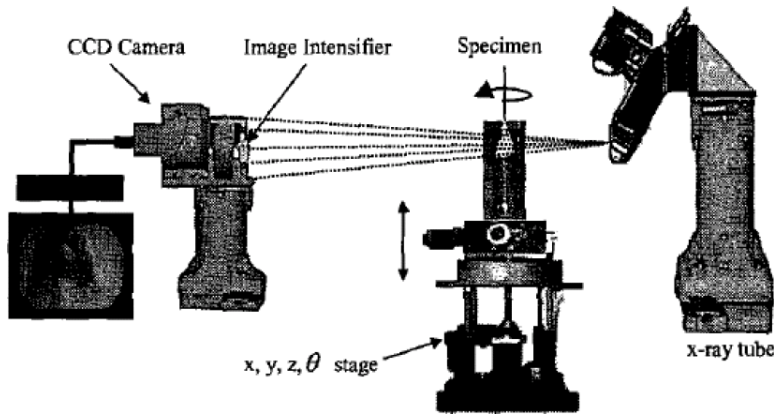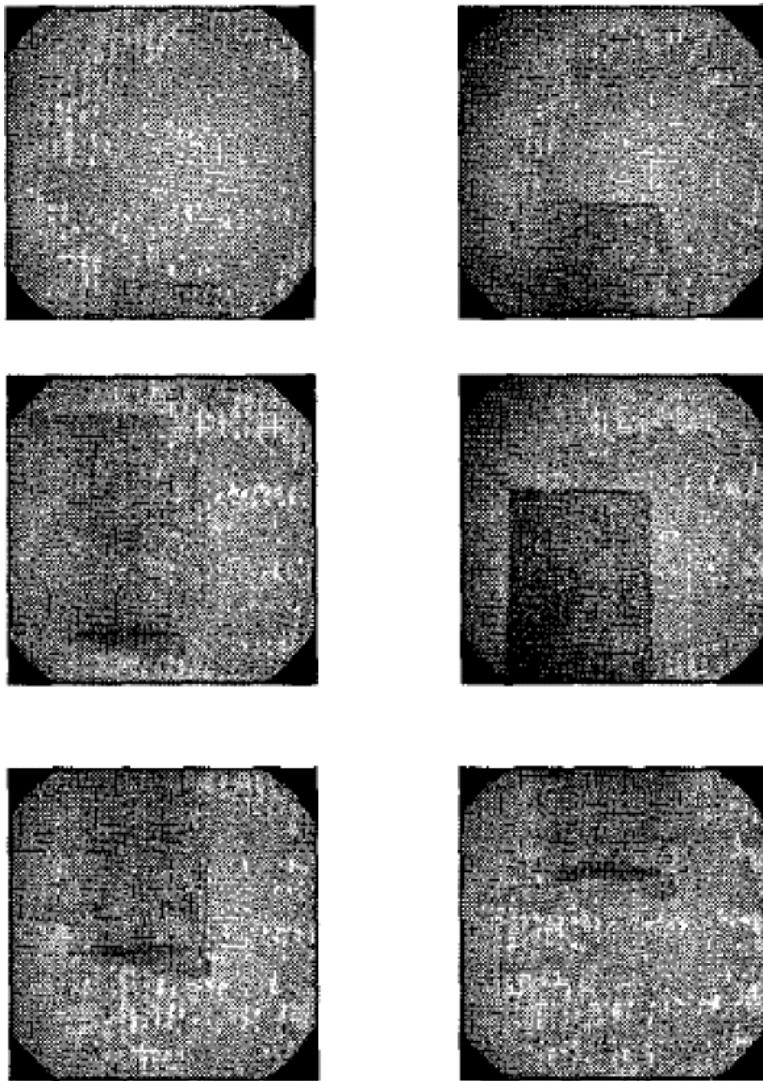
Fig. 1 Micro cone beam CT system

Fig. 2 Several representative projections for data set 1 $[\lambda_{min}, \lambda_{min} + \pi - \alpha]$

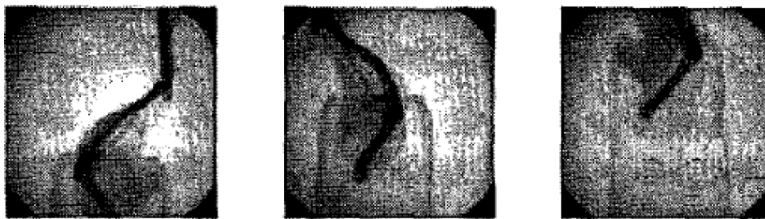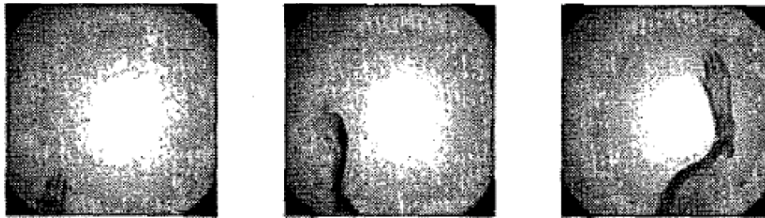**Fig. 3** Transaxial images of the reconstructed bone

Fig. 4 Several representative projections for data set 2

Fig. 5 Views from different angles of the reconstructed mouse leg

Tam[4] first provided a solution for the long object problem, but his algorithm required two circular orbits at both ends of the helix which are undesirable in practice. Several exact algorithms for the long object problem have been developed which do not require the circular orbits, but reconstruct the ROI using only the helical orbit data.[6,7,8] Although they provide good insight into the long object problem, they are very complex in implementation and computationally expensive.

In this paper, we used a simple and practical approach[1] which only needs slight modification from the implementation for the short object problem.[5]

Methods

Two truncated helical cone beam data sets are collected, The specimen for data set 1 is a chunk of bone (Fig. 2 and 3). The specimen for data set 2 is a small mouse leg (Fig. 4 and 5). The parameters used to collect data are shown on Table 1.

Table 1 Parameters used to collect data

Parameters	Data Set 1	Data Set 2
Source to iso-center distance	18 cm	12.4 cm
Source to detector distance	115 cm	57.0 cm
Detector dimension	512 x 512	512 x 512
Detector Size	14x14cm^2	14x14cm^2
Z translation per rotation	2.06 cm	3.36 cm
# of projections per rotation	360	360
Number of rotations	2	2
Effective half cone angle	1.6 degrees	3.9 degrees
Tube Voltage	62 kV	22kV
Tube Current	66 μA	358 μA

The source path $\overline{S}(\lambda)$ is a short helical segment of pitch $2\pi h$ and radius R defined by:

$2\pi h$ and radius R defined by:

$$\bar{S}(\lambda) = (R\cos\lambda, R\sin\lambda, h\lambda)^T$$

After data are collected from λ_{min} to λ_{max}, the following pseudo code is used for reconstruction.

For every projection $g(u,v,\lambda), \lambda \in [\lambda_{min}, \lambda_{max}]$

1. **Weighting**

$$g_w(u,v,\lambda) = \frac{R}{\sqrt{R^2 + u^2 + v^2}} g(u,v,\lambda) \qquad (2)$$

(u,v) is the coordinates in the 2D detector, λ is the rotation angle of the source, R is source to iso-center distance, u is parallel to the helix tangent.

2. **Filtering**

Filtered projection $g^F(u,v,\lambda)$ is a combination of a ramp filtered term $g_{ramp}(u,v,\lambda)$, a varied lower boundary term $g_{lb}(u,v,\lambda)$ and a varied upper boundary term $g_{ub}(u,v,\lambda)$

$$g^F(u,v,\lambda) = g_{ramp}(u,v,\lambda) + g_{lb}(u,v,\lambda) + g_{ub}(u,v,\lambda) \qquad (3)$$

$$g^{ramp}(u,v,\lambda) = \int du' (M_B \times g_w(u',v,\lambda))k(u-u') \qquad (4)$$

where k is the kernel of the ramp filter and M_B is the standard PI mask, its definition can be found in [5].

$g_{lb}(u,v,\lambda)$ and $g_{ub}(u,v,\lambda)$ are varied with λ and should be calculated according to Table 2 (α is the fan angle).

3. **Backprojection**

$$f(\bar{r}) = \int_{\lambda_{min}}^{\lambda_{max}} d\lambda \frac{R\sqrt{R^2 + h^2}}{\left|(\bar{r} - \bar{S}(\lambda)) \cdot (\bar{\xi}_u \times \bar{\xi}_v)\right|^2} g^F(p(\bar{r}), \lambda) \qquad (5)$$

$\bar{r}$ is a point in the object, $\bar{S}(\lambda)$ is the source orbit, $2\pi h$ is equal to the distance the X-ray source goes in one rotation, and $p(\bar{r})$ is the projection of object point $\bar{r}$ onto the detector. $\bar{\xi}_u$ and $\bar{\xi}_v$ are unit vectors in the direction of u and v, respectively.

End

The only difference between this algorithm and that for the short object problem[5] is the addition of the variable boundary term, Refer to[5,7] for detailed information on how to calculate the boundary term.

Table 2 Varied boundary term

Range of λ on the primary path	Situations of boundary term
$[\lambda_{min}, \lambda_{min} + \pi - \alpha]$	No lower boundary term
$[\lambda_{min} + \pi - \alpha, \lambda_{min} + \pi + \alpha]$	Partial lower boundary term
$[\lambda_{min} + \pi + \alpha, \lambda_{max}]$	Whole lower boundary term
$[\lambda_{max}, \lambda_{max} - (\pi - \alpha)]$	No upper boundary term
$[\lambda_{max} - (\pi + \alpha), \lambda_{max} - (\pi - \alpha)]$	Partial upper boundary term
$[\lambda_{min}, \lambda_{max} - (\pi + \alpha)]$	Whole upper boundary term

Results

Data set 1 is reconstructed on a $350*350*660$ grid. Data set 2 is reconstructed on a $378*378*686$ grid. Both specimens are reconstructed with satisfactory results. Fig. 2 shows several projections for the chunk of bone from different angles. Fig. 3 shows some transaxial images of the reconstructed bone. Fig. 4 shows several projections for the mouse leg and Fig. 5 shows volume rendering of the reconstructed mouse leg from different view angles.

Acknowledgements

References

[1]J. Hu, R. Johnson, C. Dawson, "Practical Helical Cone Beam Algorithm for the Long Object Problem", *International Meeting on Fully Three-Dimensional Image Reconstruction in Radiology and Nuclear Medicine*, Oct. 2001.

[2]J.B. Bassingthwaighte, "Back to fundamentals: anatomy-based physiological bioengineering", *Annals of Bioemedical Engieering*, vol. 28, pp. 701-703, 2000.

[3]L. A. Feldkamp, L.C. Davis, J. W. Kress, "Practical cone-beam algorithm", *J. Opt. Soc. Am. A*, vol. 1, pp. 612-619, 1984.

[4]K.C. Tam, S. Samarasekera, F. Sauer, "Exact conebeam CT with a spiral scan", *Phys. Meet. BioI*, vol. 43, pp. 1015-1024, 1998.

[5]H. Kudo, F. Noo, M. Defrise, "1998 Cone-beam filtered-backprojection algorithm for truncated helical data", *Phys. Med Biol.*, vol. 43, pp. 2885-2909.

[6]M. Defrise, F. Noo, H. Kudo, "A solution to the long object problem in helical cone beam tomography", *Phys. Med BioI*, vol. 45, pp. 1-21, 2000.

[7]H Kudo, F Noo, M Defrise, "Quasi-exact filtered backprojection algorithm for long object problem in helical cone beam tomography", *IEEE Trans. Med. Imaging*, vol. 1, pp. 902-921, 2000.

[8]S. Schaller, F. Noo, F. Sauer et al., "Exact Radon rebinning algorithm for the long object problem in helical cone beam CT", *IEEE Trans. Med. Imaging*, vol. 19, pp. 361-375, 2000.